Letter

Enhanced ionization of counter-rotating electrons via doorway states in ultrashort circularly polarized laser pulses

S. Walker, L. Kolanz, J. Venzke, and A. Becker
JILA and Department of Physics, University of Colorado, Boulder, Colorado 80309-0440, USA

(Received 10 February 2021; accepted 21 May 2021; published 7 June 2021)

We have performed single-active-electron numerical calculations of neon- and argonlike atoms interacting with short, intense, circularly polarized laser pulses at wavelengths between 10 nm and 1000 nm. Our results reveal a surprisingly large change by a factor of about 100 in the ionization ratio of electrons in initial states counter-rotating with respect to the field over corotating electrons in the previously unexplored intermediate few-photon ionization regime. The physical mechanism behind this observation is related to resonant enhanced ionization via states close in energy to the initial states. These doorway states are accessible exclusively from the initial state for counter-rotating electrons within the respective wavelength regime. The results may open a new route for controlling the generation of spin-polarized electrons by ultrashort laser pulses.

DOI: 10.1103/PhysRevA.103.L061101

Spin is an intrinsic property of electrons and plays a fundamental role in the electronic structure of all kinds of matter, ranging from atoms to solids. Ionization of a solid or gaseous atomic or molecular target with circularly polarized light is an important source of spin-polarized electrons [1]. Application of atto- or femtosecond laser pulses potentially provides the opportunity to generate ultrashort spin-polarized electron pulses for probing chiral systems and magnetic properties of materials on ultrafast timescales. A key element in the generation of spin-polarized electrons is a selectivity in ionization to the sense of the electron's rotation in the initial state with respect to the rotation direction of the laser field [2,3]. It is therefore important to identify mechanisms which increase the ionization from a specific magnetic sublevel over the others. Based on numerical solutions of the time-dependent Schrödinger equation we predict a surprisingly large enhancement in the emission of electrons, that are initially counter-rotating with respect to rotation of the applied field, during the interaction of rare-gas atoms with ultrashort circular polarized laser pulses in a previously unexplored wavelength regime. Experimental confirmation of these theoretical predictions is feasible with current intense ultrafast laser technologies.

Dependence of the depletion of the initial state on the relative rotation between electrons and field has been first demonstrated in single-photon ionization [4–6] and then in weak-field two- and three-photon ionization [7,8]. The common physical principle behind the selectivity in these early studies relies on tuning the photon energy to a Cooper minimum or specific resonances in an atom. This requirement of fine-tuning the photon energy is usually incompatible with the broad bandwidth of ultrashort laser pulses. More recently, it has been shown that, in the highly nonperturbative intensity and wavelength regime of laser-atom interaction, spin polarization of about 30%–50% can be achieved [3,9–11]. The corresponding strong-field long-wavelength propensity rule that counter-rotating electrons are easier to ionize arises from the dependence of strong-field ionization rates on the magnetic quantum number, observed both in experiment and theory [2,12–15].

The generation of spin-polarized electrons, as well as the corresponding propensity rules, in the intermediate wavelength regime of strong-field few-photon ionization remained unexplored so far. We predict that a surprisingly large change in the ionization ratio for counter- over corotating electrons from 0.1 to 10 can be expected in this wavelength regime. The maximum in the ionization from one magnetic sublevel over the other is almost an order of magnitude larger than that observed with ultrashort pulses in the tunneling regime previously. Such a strong selectivity may open new avenues towards the generation of ultrashort spin-polarized electron pulses. With our theoretical results we also address open questions concerning the transition from the short-wavelength single-photon regime, in which corotating electrons are easier to ionize, to the long-wavelength tunneling regime, where counter-rotating electrons are ionized with larger probability by a circularly polarized laser field. The physical mechanism behind our results is related to excited states which can be reached exclusively via photon absorption from the initial state with helicity opposite to that of the applied field within a certain wavelength regime. These doorway states in the electronic shell closest in energy to the ground state enable a selective enhancement of the emission of counter-rotating electrons via resonant enhanced ionization.

The mechanism that we identify as responsible for the large change in ionization ratio is different from the physical picture behind the smaller discrimination in ionization from different magnetic sublevels in the tunneling regime, where resonances do not play a role. Previous studies on the role of resonances [16–18] do not correlate with our interpretation. Peaks in helicity dependent enhancement of strong-field ionization in the deep multiphoton regime have previously been related to

resonant excitation as a general mechanism [16]. However, the crucial role of specific low-lying states acting as doorway states, that can be accessed from certain initial states only, has not been discussed before. Treating the problem in three spatial dimensions, as compared to earlier calculations in reduced dimensions, helps us to reach the conclusions presented in this study.

Our theoretical study is based on results of numerical solutions of the time-dependent Schrödinger equation corresponding to the interaction of an atom with an intense laser pulse (we use Hartree atomic units $e = m_e = \hbar = 1$ if not mentioned otherwise):

$$i\frac{\partial}{\partial t}\Psi(\mathbf{r},t) = \left[-\frac{\nabla^2}{2} + \mathbf{E}(t)\cdot\mathbf{r} + V(r)\right]\Psi(\mathbf{r},t), \qquad (1)$$

where $V(r)$ is a single-active-electron (SAE) potential for an electron in the outermost shell. In this work we have used potentials modeling $2p$ electrons in a neonlike and $3p$ electrons in an argonlike atom [19]. The vector potential of the applied field is given by

$$\mathbf{A}(t) = A_0 \sin^2\left(\frac{\pi t}{\tau}\right)[\sin(\omega t)\hat{\mathbf{x}} + \epsilon\ \cos(\omega t)\hat{\mathbf{y}}], \qquad (2)$$

where $A_0 = \frac{c\sqrt{I}}{\omega}$, $\tau = \frac{2\pi N}{\omega}$, c is the speed of light, I is the peak intensity, N is the number of cycles in the pulse, and ω is the central frequency of the vector potential. Without loss of generalization we have chosen left-handed circularly polarized pulses (i.e., $\epsilon = -1$) both in our calculations and analysis. We compare emission of electrons from all three magnetic sublevels of the p shells (i.e., $m = 0, \pm 1$) of the two atoms by applying a grid-based approach [20] as well as a numerical basis-state method (cf. [21]) to solve Eq. (1) in the three spatial dimensions. The basis-state method has been updated [22] to account for outgoing boundary conditions and improved time propagation, and results have been checked against those of the grid-based approach. Transitions to occupied states other than the initial state have been prohibited in the SAE calculations.

In our calculations we have varied the wavelength of the applied circularly polarized field from 10 nm to 1000 nm, spanning the interaction regime from single-photon ionization to tunnel ionization. We have used high peak intensity of $5 \times 10^{14}\,\mathrm{W/cm^2}$ in the case of neonlike atom (initial $2p$ states) and significantly lower intensity of $5 \times 10^{13}\,\mathrm{W/cm^2}$ for the interaction with argonlike atom (initial $3p$ states) to show that our general interpretation of the results is independent of the peak intensity of the pulse. The duration of the ultrashort pulses has been set to $N = 10$ cycles independent of wavelength. In each calculation we have prepared the atomic system in one of the three magnetic sublevels of either the $2p$ (neon) or the $3p$ shell (argon). At the end of each simulation we have determined the population in the excited states, characterized by the quantum numbers n, l, and m, via projection on the corresponding bound states of the atomic potential, which have been determined numerically. The ionization probability is then evaluated as the difference between unity and the total probability left in the bound states.

In Fig. 1 we present the probabilities of ionization P_m for the different initial magnetic sublevels $m = 0, \pm 1$ for neonlike [panel (a)] and argonlike atom [panel (b)] via the ratios P_+/P_- (stars with solid lines) and P_0/P_- (open circles with dotted lines). In both cases the ratio P_0/P_- drops stepwise at the shorter wavelengths and then continuously at the longer wavelengths. In contrast, the ratio P_+/P_- for emission of counter-rotating electrons over corotating ones shows more variation. Most interestingly in the present context is the large change in the ratio from about 0.1 to about 10 in the intermediate wavelength regime. For neonlike atom (a) the change occurs between 80 nm and 200 nm and for argonlike atom (b) between 100 nm and 300 nm. The ratios are considerably larger than those found both in the single-photon and the tunneling regime. In the intermediate wavelength regime, absorption of a few photons is required to ionize the atoms. To visualize this, we have indicated (by vertical lines) the maximum wavelengths for one-, two-, and up to five-photon ionization of the atoms. These channel closures in strong-field ionization have been determined taking into account the shift of the continuum threshold by the ponderomotive energy of the electron.

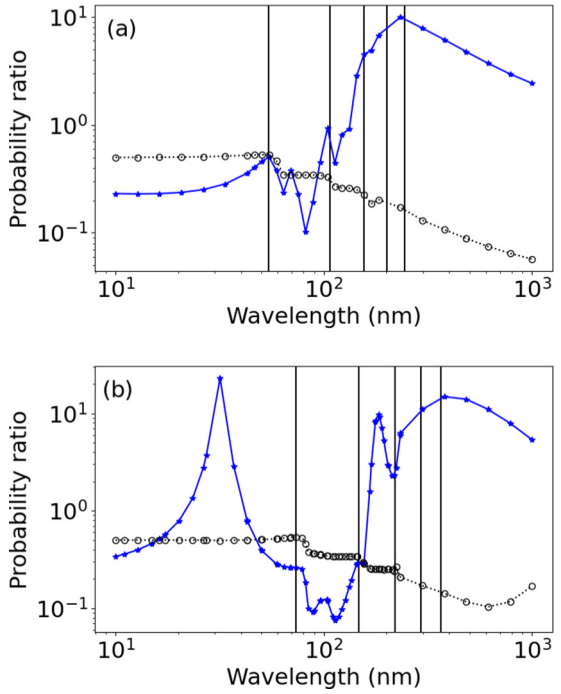

FIG. 1. Ratio P_+/P_- (stars with solid lines) and P_0/P_- (open circles with dotted lines) as function of wavelength for (a) neonlike atom ($5 \times 10^{14}\,\mathrm{W/cm^2}$) and (b) argonlike atom ($5 \times 10^{13}\,\mathrm{W/cm^2}$) interacting with 10-cycle laser pulses.

Before we analyze the surprisingly large reversal in P_+/P_- in the few-photon ionization regime, we briefly discuss other features which can be understood based on the results of earlier studies. In the single- and two-photon ionization regime our results are in agreement with those of earlier work [4,7] that, in general, corotating electrons are easier to ionize than counter-rotating ones. Similarly, at long wavelengths our results agree with earlier studies [14] that demonstrate counter-rotating electrons being ejected with higher probability in the tunneling regime. The large maximum in the single-photon regime for the argonlike atom at about 30 nm

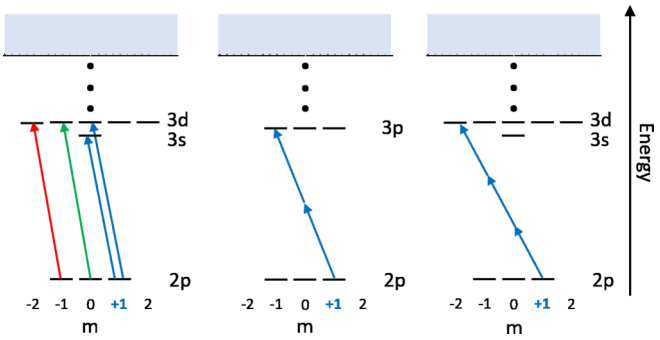

FIG. 2. One-, two-, and three-photon transitions into doorway states in the $n = 3$ shell from different initial states ($2p_1$, blue; $2p_0$, green; $2p_{-1}$, red) for ionization of neon atom with left-handed circularly polarized light ($\Delta m = -1$).

and several of the small maxima in the two-photon regime for both atoms are due to the Cooper minimum and resonant transitions, respectively. These signals are therefore short-pulse features of the effects studied for continuous lasers or long pulses in earlier studies [4,7]. The maximum near the single-photon channel closure in the neon data is due to the enhancement of s-wave photoelectron emission at small energies [23], a channel that is accessible from the initial p_{+1} levels only.

We will now turn to the physical mechanism behind the reversal in P_+/P_- and the large ratios in the few-photon ionization regime. For the general mechanism we focus on the ionization of neonlike atom (initial $2p$ states) before discussing differences specific to the argonlike atom (initial $3p$ states). The enhancement in the emission of counter-rotating electrons can be understood by considering the transitions into the sublevels closest in energy to the initial states, i.e., for neonlike atom the $n = 3$ levels. In Fig. 2 we present the allowed transitions for the three initial magnetic sublevels in the $2p$ shell. For each photon absorption from the left-handed circularly polarized field, the selection rules $\Delta l = \pm 1$ and $\Delta m = -1$ hold. For single-photon absorption (panel on left) excitation into the $n = 3$ level is allowed from each of the three magnetic sublevels. However, only counter-rotating electrons ($m = 1$) can populate both the $3s$ and the $3d$ levels, while the $3s$ level cannot be accessed from the other initial sublevels. For two- and three-photon transitions (panels in the middle and on the right, respectively) none of the levels in the $n = 3$ shell can be excited from the $m = -1$ or $m = 0$ initial sublevels. In contrast, counter-rotating electrons can be resonantly transferred either into the $3p$ or the $3d$ level, which will turn out to be the mechanism behind the large contrast in ionization yields from the magnetic sublevels.

The allowed resonant transitions are in agreement with the population distributions in the excited states of the neonlike atom at the end of the pulse at four different wavelengths (69.5 nm, 122.4 nm, 183.3 nm, and 233.6 nm from top to bottom in Fig. 3). In each panel the main part displays the distribution as function of n (vertical) and m (horizontal), summed over all possible l levels, while in the insets we present populations in certain individual states. Results for corotating electrons (initial sublevel $m = -1$) on the left and for counter-rotating electrons (initial sublevel $m = 1$) on the

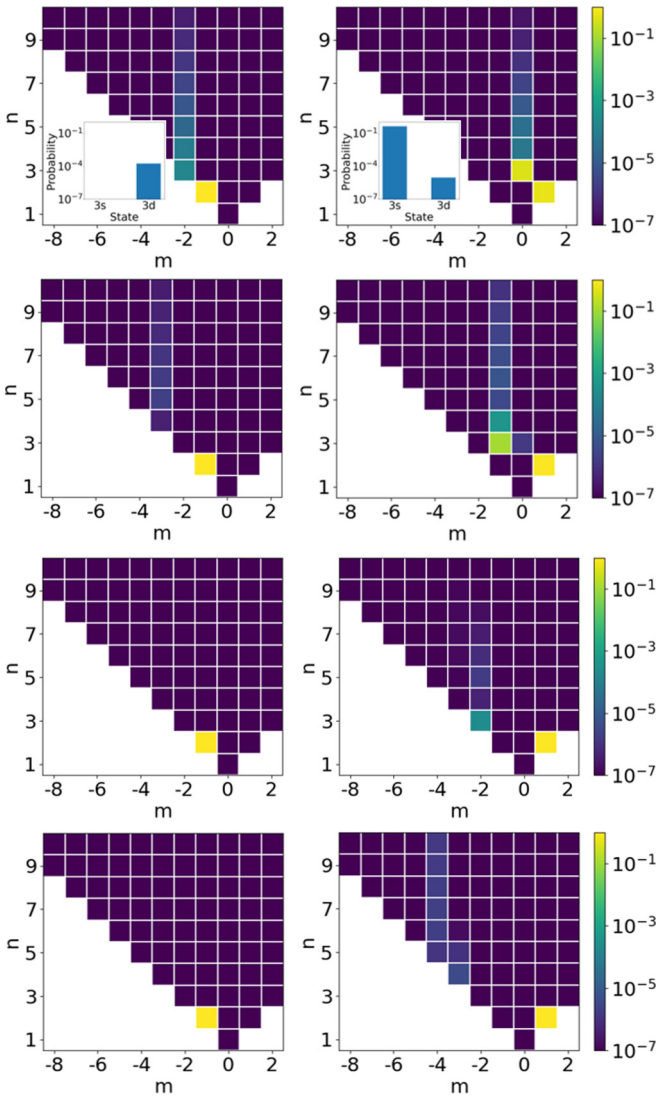

FIG. 3. Main panels: excitation probabilities as function of magnetic (m) and main (n) quantum number (summed of orbital angular momentum l) for neon atom at 69.5 nm, 122.4 nm, 183.3 nm, and 233.6 nm (from top to bottom) for initial co- ($m = -1$, left panels) and counter-rotating ($m = 1$, right panels). Insets: excitation probabilities in specific excited states.

right confirm the physical interpretation given above. At the shortest wavelength, transitions into the $n = 3$ levels lead to population in the $3s$ (for $m = 1$) and $3d$ state (for both initial states). For two- (122.4 nm) and three-photon (183.3 nm) transitions, population in the respective levels of the $n = 3$ shell are only seen for the $m = 1$ initial level. In contrast, for corotating electrons we only observe small (122.4 nm) or even no population (183.3 nm) in the higher excited states. Finally, at the longest wavelength (233.6 nm, bottom row), the $n = 3$ levels are no longer accessible from either one of the initial states while small excitation probabilities into higher excited states for $m = 1$ are still found. We note that in the calculations for the $m = 0$ initial state we have found patterns similar to those for the $m = -1$ state, in agreement with the interpretation given in the discussion of Fig. 2.

The levels in the $n = 3$ shell act as doorway states for ionization since the transition into the continuum is resonantly enhanced whenever there is a level available via photon absorption from the initial magnetic sublevels. Due to the broad spectral bandwidth of ultrashort laser pulses and the shift of energy levels during the pulses' excitations and the corresponding resonant enhanced ionization are effective not just at specific photon energies but over a broad range of wavelengths. Starting from the minimum in the P_+/P_- ratio at about 80 nm in the neonlike atom, the ratio increases at longer wavelengths due to the following effects: first, near the two-photon channel closing the enhancement via the intermediate $3s$ level, accessible for counter-rotating electrons only, becomes more effective than via the $3d$ level (cf. insets in the upper row of Fig. 3). Further increase of the wavelength ionization enhancement via resonant two- and three-photon transitions to the $n = 3$ shell, which are effective for counter-rotating electrons only, leads to the reversal of the P_+/P_- ratio until the ionization probability for counter-rotating electrons is about 10 times larger than that for corotating electrons. This enhancement is about an order of magnitude larger than that observed in the tunneling regime before. Beyond the maximum, at about 250 nm, the ratio drops again for each initial sublevel since resonant transitions become less effective due to the large number of photons needed to reach the accessible highly excited states. Consistently, we have found a significant decrease in the overall excitation probabilities for all initial magnetic sublevels at these wavelengths. We note that the interpretation of the significance of resonant enhanced ionization via doorway states is also consistent with the results for P_0/P_- in Fig. 1(a), since the general accessibility of levels in the $n = 3$ shell is the same for the initial $m = -1$ and $m = 0$ levels (cf. Fig. 2). The P_0/P_- ratio scales with the number of photons absorbed in the ionization process.

In general, the results for an argonlike atom in Fig. 1(b) can be interpreted in the same way as those for the neonlike atom. A few additional features arise due to the more complex level structure among the doorway states closest in energy to the initial $3p$ levels. Besides the unoccupied $3d$ level, one needs to consider the $4f$ level as well. Effects can be seen in the excitation probabilities at the end of the pulse at 112.9 nm and 169.1 nm in Fig. 4 (upper row). Due to the resonant enhancement of counter-rotating electrons via the $4s$- and $4p$-doorway states the ratio P_{+1}/P_{-1} rises from the minimum to the first maximum in the intermediate wavelength regime in Fig. 1(b). The following decrease in the ratio up to 210 nm can be explained by the fact that the $4p$ channel closes before the next doorway states ($4d$ and $4f$) become accessible for the counter-rotating electrons (lower row of Fig. 4). The overall enhanced populations for the counter-rotating electrons (blue columns) in the low-lying excited states, as compared to those for the corotating ones (red columns), reflect the importance of these doorway states for the large change in the P_+/P_- ratio. Once all these doorway states are closed for both co- and counter-rotating electrons at even longer wavelengths, resonant transitions become less effective and the ratio of the ionization probabilities decreases towards its limit in the tunneling regime, as in the case for the neonlike atom. The physical picture behind the selectivity in ionization in the tunneling regime is different than the mechanism identified in the present work, since excited states and resonances do not play a role in tunneling ionization. In general, the role of each individual photon absorption is insignificant in the tunneling regime, which can be considered as a limit when the number of photons involved is large [24].

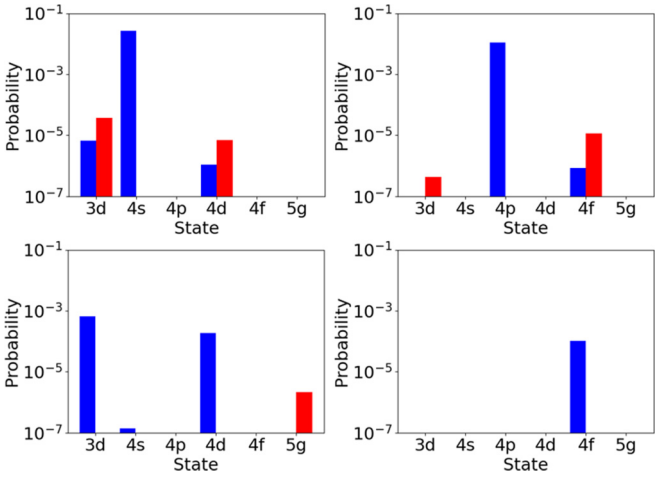

FIG. 4. Excitation probabilities in specific excited states of argon atom at 112.9 nm (upper left), 169.1 nm (upper right), 233.6 nm (lower left), and 297.6 nm (lower right) for initial states with co- ($m = -1$, red) and counter-rotating electrons ($m = 1$, blue).

To summarize, our numerical results for the ionization from different magnetic sublevels in rare-gas-like atoms by ultrashort, intense, circularly polarized pulses indicate a surprisingly large change by a factor of about 100 in the ratio of ionization of counter- over corotating electrons in the few-photon ionization regime. The enhancement in the emission from the initial sublevel with counter-rotating electrons is due to resonant enhanced ionization via states close in energy to the initial states. In the corresponding wavelength regime these doorway states are accessible only when the applied field is counter-rotating with respect to the initial magnetic sublevel. The present theoretical results may also help to further understand previous experimental data obtained in xenon atom with laser light at about 400 nm [10,11], which show a high degree of spin polarization.

This work was primarily supported by a grant from the U.S. Department of Energy, Division of Chemical Sciences, Atomic, Molecular and Optical Sciences Program (Award No. DE-SC0001771). We also acknowledge a grant from the U.S. National Science Foundation (Grant No. PHY-1734006) for computer resources used for part of the present calculations.

[1] J. Kessler, *Polarized Electrons* (Springer, Berlin, 1985).

[2] I. Barth and O. Smirnova, Phys. Rev. A **84**, 063415 (2011).

[3] A. Hartung, F. Morales, M. Kunitski, K. Henrichs, A. Laucke, M. Richter, T. Jahnke, A. Kalinin, M. Schöffler, L. P. H. Schmidt *et al.*, Nat. Photon. **10**, 526 (2016).

[4] U. Fano, Phys. Rev. **178**, 131 (1969).
[5] G. Baum, M. S. Lubell, and W. Raith, Phys. Rev. Lett. **25**, 267 (1970).
[6] U. Heinzmann, J. Kessler, and J. Lorenz, Phys. Rev. Lett. **25**, 1325 (1970).
[7] P. Lambropoulos, Phys. Rev. Lett. **30**, 413 (1973).
[8] E. H. A. Granneman, M. Klewer, K. J. Nygaard, and M. J. V. d. Wiel, J. Phys. B: At. Mol. Phys. **9**, L87 (1976).
[9] I. Barth and O. Smirnova, Phys. Rev. A **88**, 013401 (2013).
[10] M.-M. Liu, Y. Shao, M. Han, P. Ge, Y. Deng, C. Wu, Q. Gong, and Y. Liu, Phys. Rev. Lett. **120**, 043201 (2018).
[11] D. Trabert, A. Hartung, S. Eckart, F. Trinter, A. Kalinin, M. Schöffler, L. Ph. H. Schmidt, T. Jahnke, M. Kunitski, and R. Dörner, Phys. Rev. Lett. **120**, 043202 (2018).
[12] T. Herath, L. Yan, S. K. Lee, and W. Li, Phys. Rev. Lett. **109**, 043004 (2012).
[13] I. Barth and O. Smirnova, Phys. Rev. A **87**, 013433 (2013).
[14] I. Barth and M. Lein, J. Phys. B: At., Mol., Opt. Phys. **47**, 204016 (2014).
[15] S. Eckart, M. Kunitski, M. Richter, A. Hartung, J. Rist, F. Trinter, K. Fehre, N. Schlott, K. Henrichs, L. P. H. Schmidt *et al.*, Nat. Phys. **14**, 701 (2018).
[16] X. Zhu, P. Lan, K. Liu, Y. Li, X. Liu, Q. Zhang, I. Barth, and P. Lu, Opt. Express **24**, 4196 (2016).
[17] J. H. Bauer and Z. Walczak, Phys. Rev. A **101**, 063409 (2020).
[18] S. Xu, Q. Zhang, X. Fu, X. Huang, X. Han, M. Li, W. Cao, and P. Lu, Phys. Rev. A **102**, 063128 (2020).
[19] R. Reiff, T. Joyce, A. Jaron-Becker, and A. Becker, J. Phys. Commun. **4**, 065011 (2020).
[20] J. Venzke, A. Jaron-Becker, and A. Becker, J. Phys. B: At., Mol., Opt. Phys. **53**, 085602 (2020).
[21] S. Chen, X. Gao, J. Li, A. Becker, and A. Jaron-Becker, Phys. Rev. A **86**, 013410 (2012).
[22] S. Walker, A. Jaron-Becker, and A. Becker (unpublished).
[23] B. Bransen and C. Joachain, *Physics of Atoms and Molecules* (Addison-Wesley, Redwood City, CA, 2003).
[24] A. Becker and F. H. M. Faisal, J. Phys. B: At., Mol., Opt. Phys. **38**, R1 (2005).